Scientific
Research

Structural and Morphological Study of a Series of Ball Milled Nanocrystalline $Fe_{1-x}Al_x$ ($0.3 \leq x \leq 0.6$) Alloys

Sandeep Rajan[1], Rajni Shukla[1], Anil Kumar[2], Anupam Vyas[2], Ranjeet Brajpuriya[2*]

[1]Department of Physics, Deenbandhu Chhotu Ram University of Science & Technology, Murthal, India
[2]Department of Physics, Amity University Haryana, Manesar, India
Email: [*]ranjeetbjp@yahoo.co.in

Abstract

In the present manuscript, the authors have systematically investigated the structural and morphological properties of a series of mechanically alloyed $Fe_{1-x}Al_x$ ($0.3 \leq x \leq 0.6$) samples using X-Ray Diffraction (XRD) and Scanning Electron Microscopy (SEM). All the samples, after 5 hr of milling, show crystalline structure, irrespective of the constituent concentration and are textured mainly along (110) direction. In Fe-rich samples, the formation of an off-stoichiometric Fe_3Al phase is favored and in case of Al-rich samples, both Al-rich phases and clustering of Al atoms are present. Analysis of line breadths was carried out to get an insight into the interrelated effects of average crystallite size, and lattice parameters. The grain size of constituents was decreased to the nanometer range (between 6 - 8 nm) and the constituents dissolved at the nanograin boundaries. Similar conclusions were also revealed from the SEM results which show that the initial shape of particles disappeared completely, and their structure became a mixture of small and large angular-shaped crystallites with different sizes. The results of this research could be directly employed in the design of deformation schedules for the industrial processing of Fe-Al alloys.

Keywords

Intermetallics, FeAl, Phase Formation, XRD, SEM, Mechanical Alloying

1. Introduction

Magnetic nanogranular systems, formed by embedding magnetic grains or clusters (few nanometer in size), in a magnetic or nonmagnetic matrix, are an important class of nanostructured magnetic materials. The matrix can be

---
[*]Corresponding author.

metallic or insulating, crystalline or amorphous and can correspond to either the grain boundary regions or to a phase with structure or composition different from that of the magnetic phase [1]. In these systems, the surface to volume ratio of the crystallites is extremely high due to nanometric dimensions of the crystallites. This leads to interesting magnetic properties which are significantly different from that of the bulk.

The FeAl intermetallic is considered as a potential high-temperature structural material due to its attractive physical and mechanical properties, such as high melting point, low density, high thermal conductivity and excellent oxidation resistance [2] [3]. However, its practical application is restricted due to its inherent poor ductility and toughness, especially at ambient temperatures [4] [5]. In order to overcome this drawback, considerable attempts have been carried out, such as thermomechanical processing, micro-alloying and macro-alloying [6] [7]. Additionally, the preparation of fine-grained material is also a feasible approach to improve the room-temperature ductility, since brittle material may be transformed into ductile material by grain refinement [8] [9]. Nanocrystalline intermetallic compounds are said to have enhanced ductility and yield strength as compared to conventional grain-sized materials [10], and mechanical alloying in ball mills has been considered a suitable processing method capable of attaining the goal of producing nanostructured materials [11]. Not only mechanical alloying is capable of reducing grain size but it can also lead to the following changes in the material: disordering of the lattice and modification of the crystalline structure of crystals into a more symmetric [11]. It is well-known that the mechanical and magnetic properties of these systems are intimately related to the microstructure and the degree of disorder in the system [12].

The type of structures and phases formed are very sensitive to the Fe to Al content. Iron-aluminum phase diagram [13] exhibits several intermetallic phases at varying compositions and temperatures, two ordered phases, namely the B2 and DO_3 pre-dominate the field with stability over a wide range of composition. However, use of a non-equilibrium process like mechanical alloying results in the formation of intermediate magnetic phases. Along with nanostructuring and disordering, the presence of these intermediate phases would lead to interesting bulk and microscopic magnetic properties. Both from the point of view of understanding the collective behaviour of the magnetic phases and also possible applications, study of such intermediate phases is expected to be very rewarding. With this objective, in the present work, we have systematically studied the structural evolution of Fe-Al powders mixed in the different compositions by high energy MA treatment for 5 hr. In particular, we have focused our attention on the mechanisms of formation of a solid solution obtained after long time of MA, to the diffusivity of Al in the Fe-Al solid solution, and to the interface mobility in the FeAl intermetallic. The experimental techniques used for the elemental characterization, phase transformation, changes in structural properties, morphology and grain size of mechanically alloyed powder are X-Ray Diffraction (XRD) and Scanning Electron Microscopy (SEM).

2. Experimental Details

The alloys with series of $Fe_{1-x}Al_x$ ($0.3 \leq x \leq 0.6$) were prepared by high-energy MA of analytical grade Fe and Al powders of approximately 300 mesh sizes and with purities of 99.9%. The powders were initially mixed thoroughly using agate pestle and mortar and then dry-milled in argon atmosphere using a SPEX 8000 M high-energy mixer/mill with hardened steel vials and balls for a fixed time of 5 hr. To avoid excessive heating during milling, each 30 min of milling was followed by a pause of 45 min under Ar atmosphere. Micro-structural characterization of the milled powders was performed by using a Bruker D-8 Advance X-ray diffractometer with Cu Kα radiation. The wavelength of the X-Ray used was 0.154 nm. The average crystallite size $\langle D \rangle$ was calculated from the broadening of X-Ray diffraction peaks. Scanning Electron Microscope (SEM) was used for crystallite size measurements and to study the morphology of the mechanically alloyed powder samples. The investigation into milling media and atmospheric contaminations were also done by utilizing the EDAX facility.

3. Result and Discussion

Figure 1 shows the x-ray diffractograms of $Fe_{1-x}Al_x$ ($0.3 \leq x \leq 0.6$) powders subjected to high-energy mechanical alloying for a fixed period of 5 hrs. From **Figure 1**, one can perceive phase transformations occurring in the powder samples as a result of mechanical milling. The XRD pattern for the starting powder (labeled unmilled) shows reflections corresponding to distinct bcc Fe and fcc Al metals. Other than Al (111), Al (200) and (220) peaks overlap with Fe (110) and (200) peaks. However, after milling it is found that the XRD patterns of the
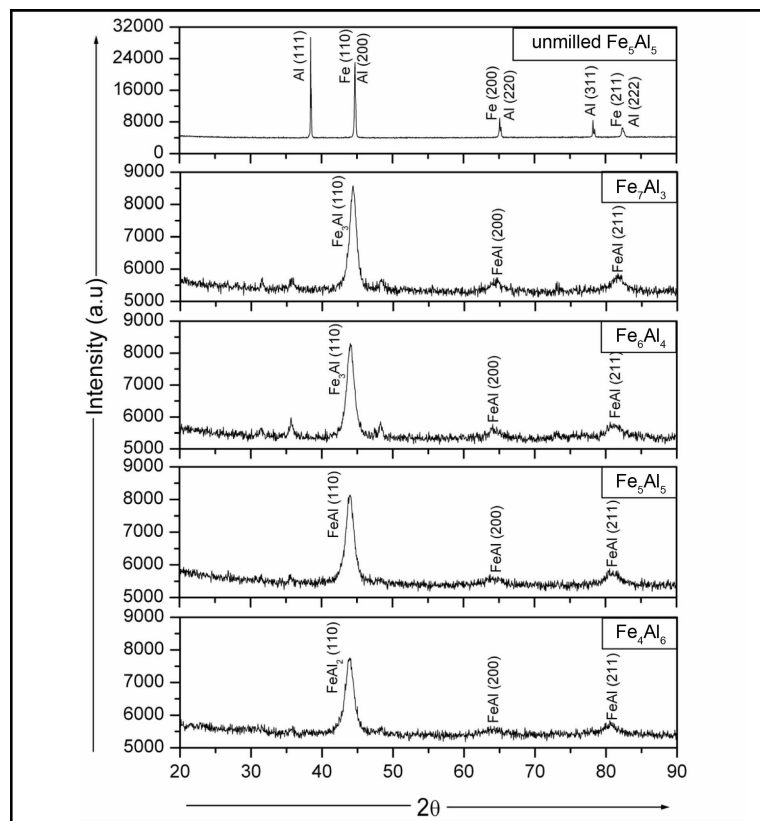
Figure 1. XRD patterns of unmilled and 5 hrs ball milled $Fe_{1-x}Al_x$ alloys.

FeAl alloy samples do not match any of the XRD peaks of elemental Fe or Al powder particles. The first major effect of milling is the decrease in intensity of the Fe & Al peaks and their disappearance at longer milling times. After 5 hr of milling, the reflection peaks corresponding to fcc Al (at $2\theta = 39.3°$) of Al (111) disappeared completely due to complete dissolution of Al in to Fe, indicating the formation of Fe(Al) solid solution. In the same time period, the main Fe peak becomes asymmetric and very broad due to refinement of crystallite size as well as enhancement in internal strain. Both these effects are caused by severe plastic deformation of powder particles during milling process due to impact force of colliding balls. Further all the samples after MA for 5 hours, show crystalline structure and textured mainly along (110) direction, irrespective of the Al content. The high intensity peak at $2\theta = 44.25°$ corresponds to FeAl (110) and the other low intensity peaks are due to the reflections from FeAl (100), FeAl (200) and FeAl (211) planes, respectively. After deep study of the graph we have seen an appearance of a new peak at 31.6° with small intensity which clearly indicates the structural transformation & formation of bcc Fe(Al) solid solution, as this peak is absent for elemental bcc Fe or fcc Al.

As already discussed the fundamental peaks in the X-ray spectra are found to broaden due to reduction in crystallite size and increase in internal strain. Taking into account the effect of strain on the broadening of peaks, the average crystallites size of all the samples are obtained using Scherrer formalism is shown in **Table 1**. It is found that the crystallite size decreases drastically as compared to unmilled samples and also with respect to *x*. This is due to both, increase in amorphization as well as the formation of disordered Fe-rich FeAl alloy (*i.e.* Fe_3Al) phases at lower x and Al-rich FeAl alloy phases at higher *x*.

It is also seen from **Figure 1**, that the fundamental peaks are consistently broadened and shifted to lower angles with increase in *x*. The shifting of the fundamental peaks to lower angles indicates an expansion of the lattice and presence of internal strain occurs as a result of non-uniform alloy formation during sample preparation. The variation in lattice parameter (a_0) as a function of x is shown in **Table 1**. Also the relative reduction in the integrated intensity (I) of the FeAl (110) peak as a function of x (see **Table 1**) further supports the FeAl alloy formation.

Since 2θ values of the existing phases of FeAl namely, Fe_3Al (DO3), FeAl (B2), $FeAl_2$ and Fe_2Al_5 are almost

overlapping, and it is therefore difficult to conclude from these results about which phase selectively will form. Also from the thermodynamics point of view, we cannot derive the conclusions because the heat of formation of the Al-rich phases has quite similar values to that of the B2 phase [14]. However, from the atomic composition point of view, we may conclude the formation of an off-stoichiometric Fe_3Al phase in the Fe-rich samples, while the Al-rich compositions have both Al-rich phases and clustering of Fe atoms, respectively.

The powder morphology of the samples was studied by SEM. **Figure 2** shows the morphological evolution of $Fe_{1-x}Al_x$ alloy samples as a function of x. For the unmilled powder (**Figure 2(a)**), the existence of iron particles (spherical in shape with an average particle size of 2.5 μm) and Al particles (irregular lamellar structure with an average particle size of 3.5 μm) are clearly observed. As a result of intensive fracture and cold welding during the ball milling, the structure and shape of the particles have been changed drastically as shown in **Figures 2(b)- (f)**. **Figure 2(b)** depicts the morphology of $Fe_{0.7}Al_{0.3}$ alloy sample milled for 5 hr. One can clearly see that the

Table 1. Structural parameters of $Fe_{1-x}Al_x$ alloy samples as a function of x.

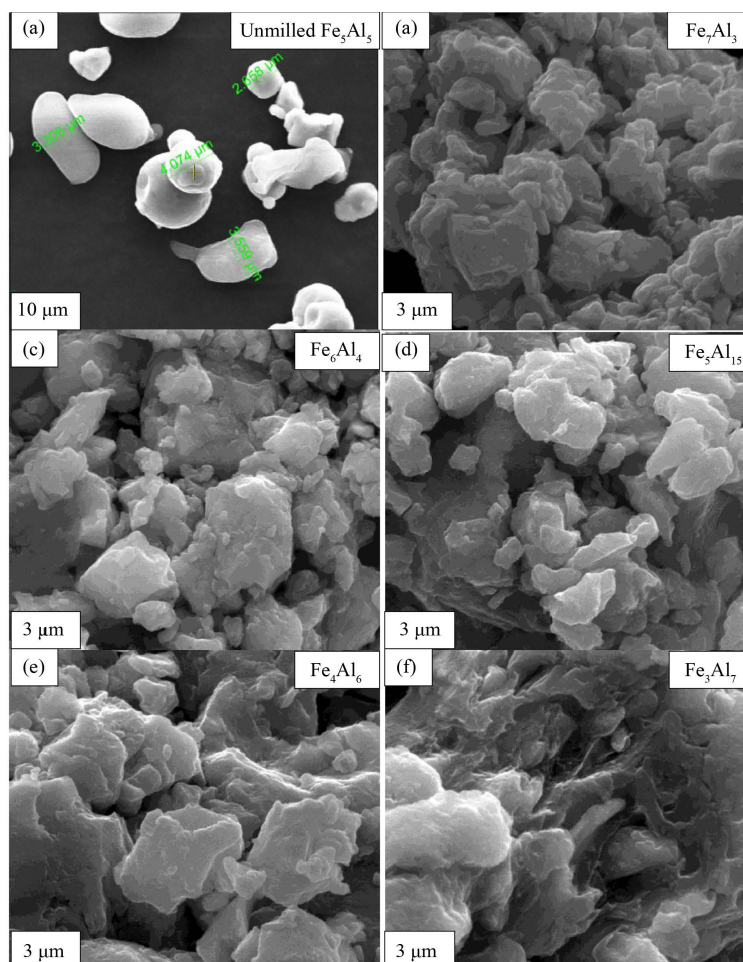| Sample $Fe_{1-x}Al_x$	Crystallite Size $\langle D \rangle$ in nm	Lattice Parameter (a_0) in nm	Intensity (I) in %
$x = 0.3$	7.5	0.289	100
$x = 0.4$	7.2	0.290	92
$x = 0.5$	6.2	0.291	82
$x = 0.6$	6.0	0.292	62

Figure 2. SEM micrographs of unmilled Fe & Al powder and 5 hr ball milled $Fe_{1-x}Al_x$ alloys.

initial shape of crystallites disappeared completely, and their structure became an amalgam of small and large irregular and angular shaped particles with wide range of sizes. During ball milling, the grain size of constituents was decreased to the nanometer range and the constituents dissolved at the nanograin boundaries, which provided the strong conditions for the solid-state synthesis reaction. This phenomenon is a result of the existence of a balance between the fracture and re-welding processes. Mechanical Alloying (MA) is a solid-state powder processing technique involving repetitive action of plastic deformation under shocks, welding into sandwiches between two or more elemental components and subsequent breaking and re-welding. With increasing milling time the layers become finer and finer and finally thicknesses of nanometric or even interatomic distances are achieved. This extremely low layer thickness together with substantial increase in temperature due to shocks between colliding balls helps solid state reactions to occur.

The formation of FeAl intermetallic alloy from elemental Fe and Al powders appears to be composed of two steps: progressive refinement of Fe and Al grains within the sandwich type microstructure, followed by FeAl formation, presumably at the interfaces between Fe and Al grains. However, with increase in x, further welding and flattening of the particles are observed as seen from **Figures 2(c)-(f)**. Particularly in Al rich composition *i.e.* $Fe_{0.3}Al_{0.7}$ one can see the flattening of crystallites more of a disordered layered structure. From SEM images, it is clear that the iron and aluminium elemental distributions are closely correlated indicating that the two elements are completely alloyed and the FeAl solid solution is formed. These results are very consistent with the XRD analysis. Further information is obtained with the help of Energy dispersive X-ray (EDAX) analysis, made on all samples. **Figure 3** shows energy dispersive X-ray (EDAX) analysis on a particle mechanically alloyed for 5 hrs, approximately an average composition of Fe-50 at % Al is obtained as indicated in **Table 2**. The EDAX analysis showed only Fe and Al peaks, and no tungsten, oxygen and carbon peaks are seen in **Figure 3**, suggesting negligible contamination from the atmosphere and the milling media. EDAX and XRD results are similar with respect to phase transformation, particle size and contamination, thus showing consistency in the investigated results.

Table 2. Results of EDAX performed using SEM on a 5-hr mechanically alloyed $Fe_{0.5}Al_{0.5}$ alloy sample.

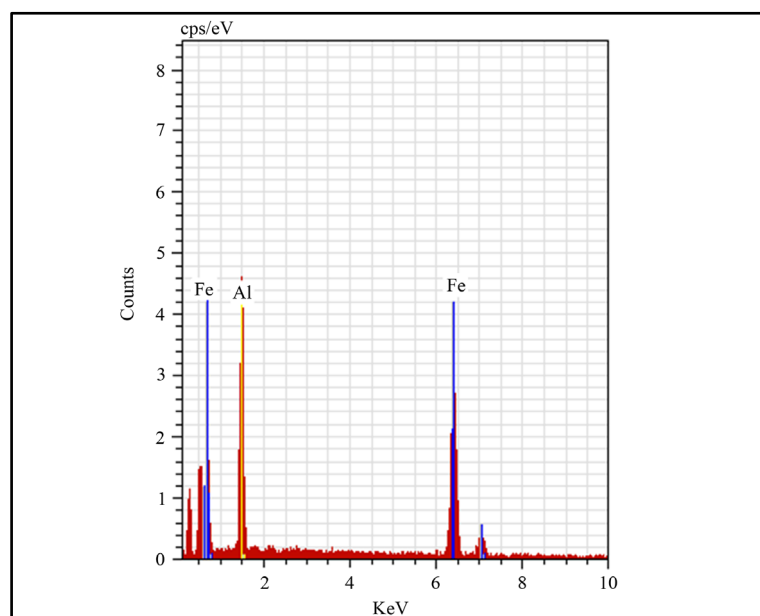| Elements	KeV	Mass %	Atomic %	Error %
Fe Kα	6.40	67.58	50.18	1.5
Al Kα	1.49	32.42	49.82	1.2
Total		100	100	

Figure 3. EDAX graph indicates Fe and Al peaks.

4. Conclusion

In conclusion, a systematic study of the structural and morphological properties of $Fe_{1-x}Al_x$ ($0.3 \leq x \leq 0.6$) samples shows that in the Fe-rich samples, formation of an off-stoichiometric Fe_3Al phase is favored and in case of Al-rich samples both Al-rich phases and clustering of Al atoms are present. All the samples are textured mainly along (110) direction and show crystalline structure, irrespective of the constituent concentration and the grain size of constituents was decreased to the nanometer range. This system is further suited for magnetization study, to understand the nature of exchange interactions involved.

Acknowledgements

References

[1] Hernando, A. and Gonzalez, J.M. (2000) *Hyperfine Interactions*, 1**30**, 221-240. http://dx.doi.org/10.1023/A:1011096522429

[2] Deevi, S.C. and Sikka, V.K. (1996) *Intermetallics*, **4**, 357-375. http://dx.doi.org/10.1016/0966-9795(95)00056-9

[3] Kouvel, J.S., Westbrook, J.H. and Fleischer, R.L. (1994) Intermetallic Compounds: Principles. Wiley, New York.

[4] George, E.P., Yamaguchi, M., Kumar, K.S. and Liu, C.T. (1994) *Annual Review of Materials Science*, **24**, 409-451. http://dx.doi.org/10.1146/annurev.ms.24.080194.002205

[5] Deevi, S.C. (2000) *Intermetallics*, **8**, 679-685. http://dx.doi.org/10.1016/S0966-9795(99)00129-6

[6] Pocci, D., Tassa, O. and Testani, C. (1994) Processing Properties and Applications of Iron Aluminides. In: Schneibel, J.H. and Crimp, M.A., Eds., *The Materials*, *Metals and Minerals Society*, Warrendale, 19-30.

[7] Srinivasan, M.N. and Sikka, V.K. (1994) Tensile Properties of a Mechanically Alloyed Fe_3Al-Based Alloy. In: Schneibel, J.H. and Crimp, M.A., Eds., *Processing*, *Properties and Applications of Iron Aluminides*, The Minerals, Metals and Materials Society, Warrendale, 69-78.

[8] Gleiter, H. (1991) *Progress in Materials Science*, **33**, 223-315. http://dx.doi.org/10.1016/0079-6425(89)90001-7

[9] Koch, C.C. (1992) *Materials Science Forum*, **243**, 88-90.

[10] Bohn, R., Haubold, T., Birringer, R. and Gleiter, H. (1991) *Scripta Metallurgica et Materialia*, **25**, 811-816. http://dx.doi.org/10.1016/0956-716X(91)90230-X

[11] Suryanarayana, C. (2001) *Progress in Materials Science*, **46**, 1-184. http://dx.doi.org/10.1016/S0079-6425(99)00010-9

[12] Hernando, A., Amils, X., Nogues, J., Surinach, S., Baro, M.D. and Ibarra, M.R. (1998) *Physical Review B*, **58**, Article ID: R11864.

[13] Kattner, U.R. (1990) Binary Alloy Phase Diagrams. In: Massalski, T.B., Ed., ASM International, Metals Park, 147.

[14] Hultgren, R., *et al*. (1973) Selected Values of the Thermodynamic Properties of Binary Alloys. American Society for Metals, Metals Park, 156.